

COURSE 1

**NUCLEAR MAGNETIC RESONANCE QUANTUM  
COMPUTATION**

J. A. JONES

*Centre for Quantum Computation,  
Clarendon Laboratory, Parks Road,  
Oxford OX1 3PU, UK*

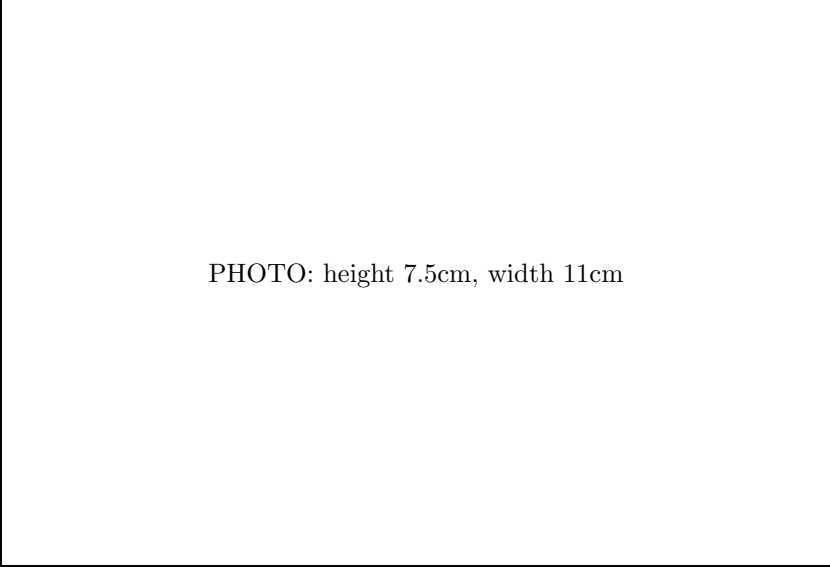


PHOTO: height 7.5cm, width 11cm

## Contents

<b>1 Nuclear Magnetic Resonance</b>	<b>3</b>
1.1 Introduction . . . . .	3
1.2 The Zeeman interaction and chemical shifts . . . . .	4
1.3 Spin-spin coupling . . . . .	5
1.4 The vector model and product operators . . . . .	6
1.5 Experimental practicalities . . . . .	8
1.6 Spin echoes and two-spin systems . . . . .	9
<b>2 NMR and quantum logic gates</b>	<b>10</b>
2.1 Introduction . . . . .	10
2.2 Single qubit gates . . . . .	11
2.3 Two qubit gates . . . . .	12
2.4 Practicalities . . . . .	13
2.5 Non-unitary gates . . . . .	15
<b>3 NMR quantum computers</b>	<b>17</b>
3.1 Introduction . . . . .	17
3.2 Pseudo-pure states . . . . .	18
3.3 Efficiency of NMR quantum computing . . . . .	20
3.4 NMR quantum cloning . . . . .	21
<b>4 Robust logic gates</b>	<b>24</b>
4.1 Introduction . . . . .	25
4.2 Composite rotations . . . . .	25
4.3 Quaternions and single qubit gates . . . . .	27
4.4 Two qubit gates . . . . .	29
4.5 Suppressing weak interactions . . . . .	30
<b>5 An NMR miscellany</b>	<b>31</b>
5.1 Introduction . . . . .	31
5.2 Geometric phase gates . . . . .	32
5.3 Limits to NMR quantum computing . . . . .	34
5.4 Exotica . . . . .	35
5.5 Non-Boltzmann initial states . . . . .	37
<b>6 Summary</b>	<b>38</b>
<b>A Commutators and product operators</b>	<b>38</b>

# NUCLEAR MAGNETIC RESONANCE QUANTUM COMPUTATION

J. A. Jones

## Abstract

Nuclear Magnetic Resonance (NMR) is arguably both the best and the worst technology we have for the implementation of small quantum computers. Its strengths lie in the ease with which arbitrary unitary transformations can be implemented, and the great experimental simplicity arising from the low energy scale and long time scale of radio frequency transitions; its weaknesses lie in the difficulty of implementing essential non-unitary operations, most notably initialisation and measurement. This course will explore both the strengths and weaknesses of NMR as a quantum technology, and describe some topics of current interest.

## 1 Nuclear Magnetic Resonance

Before describing how Nuclear Magnetic Resonance (NMR) techniques can be used to implement quantum computation I will begin by outlining the basics of NMR.

### 1.1 Introduction

Nuclear Magnetic Resonance (NMR) is the study of the direct transitions between the Zeeman levels of an atomic nucleus in a magnetic field [1–7]. Put so simply it is hard to see why NMR would be of any interest<sup>1</sup>, and the field has been largely neglected by physicists for many years. It has, however, been adopted by chemists, who have turned NMR into one of the most important branches of chemical spectroscopy [8].

Some of the importance of NMR can be traced to the close relationship between the information which can be obtained from NMR spectra and the

---

<sup>1</sup>The interest in and importance of NMR is hinted at by the fact that research into NMR has led to Nobel prizes in Physics (Bloch and Purcell, 1952), Chemistry (Ernst, 1991, and Wütrich, 2002) and Medicine (Lauterbur and Mansfield, 2003).

information about molecular structures which chemists wish to determine, but an equally important factor is the enormous sophistication of modern NMR experiments [3], which go far beyond simple spectroscopy. The techniques developed to implement these modern NMR experiments are essentially the techniques of coherent quantum control, an area in which NMR exhibits unparalleled abilities. It is, of course, this underlying sophistication which has led to the rapid progress of NMR implementations of quantum computing.

The basis of NMR quantum computing will be described in subsequent lectures, but I will begin by outlining the ideas and techniques underlying conventional NMR experiments. This is important, not only to gain an understanding of the key physics behind NMR quantum computing, but also to understand the language used in this field. Throughout these lectures I will use the Product Operator notation, which is almost universally used in conventional NMR [2, 6, 9–11]. Although ultimately based on traditional treatments of spin physics this notation differs from the usual physics notation in a number of subtle ways.

## 1.2 *The Zeeman interaction and chemical shifts*

Most atomic nuclei possess an intrinsic angular momentum, called spin, and thus an intrinsic magnetic moment. If the nucleus is placed in a magnetic field the spin will be quantised, with a small number of allowed orientations with respect to the field. For both conventional NMR and NMR quantum computing the most important nuclei are those with a spin of one half: these have two spin states, which are separated by the Zeeman splitting

$$\Delta E = \hbar\gamma B \quad (1.1)$$

where  $B$  is the magnetic field strength at the nucleus and  $\gamma$ , the gyromagnetic ratio, is a constant which depends on the nuclear species. Among these spin-half nuclei the most important species [5] are  $^1\text{H}$ ,  $^{13}\text{C}$ ,  $^{15}\text{N}$ ,  $^{19}\text{F}$  and  $^{31}\text{P}$ .

Transitions between the Zeeman levels can be induced by an oscillating magnetic field with a resonance frequency  $\nu = \Delta E/h$  (the Larmor frequency). As the Larmor frequency depends linearly on the magnetic field strength it is usually desirable to use the strongest magnetic fields conveniently available. This is achieved using superconducting magnets, giving rise to fields in the range of 10 to 20 Tesla. For  $^1\text{H}$  nuclei, which are the most widely studied by conventional NMR, the corresponding resonance frequencies are in the range of 400 to 800 MHz, lying in the radiofrequency (RF) region of the spectrum, and the field strengths of NMR magnets are usually described by stating the  $^1\text{H}$  resonance frequency.

The relatively low frequency of NMR transitions has great significance for NMR experiments. The energy of a radio frequency photon (about 1

$\mu\text{eV}$ ) is so low that it is essentially impossible to detect single photons, and it is necessary to use fairly large samples (around 1 mg) containing an ensemble of about  $10^{19}$  identical molecules. Even then the signal is weaker than one might hope, as the nuclei are distributed between the upper and lower energy levels according to the Boltzmann distribution, and the population excess in the lower level is less than 1 in  $10^4$ .

From the description above one would expect all the  $^1\text{H}$  nuclei in a sample to have the same resonance frequency, but in fact variations are seen. These arise from the *chemical shift* interaction [6], which causes the magnetic field strength experienced by the nucleus to differ from that of the applied field. Atomic nuclei do not occur in isolation, but are surrounded by electrons, and the applied field will induce circulating currents in the electron cloud; these circulating currents cause local fields which will combine with the applied field to give a total field which determines the NMR frequency. Clearly the local fields will depend on the nature of the surrounding electrons, and thus on the chemical environment of the nucleus. Chemical shifts can in principle be calculated using quantum mechanics, but in practice it is more useful to interpret them using semi-empirical methods developed by chemists [5].

Three further points about chemical shifts should be considered. Firstly the strength of the induced fields depends linearly on the strength of the applied field, and so chemical shifts measured as frequencies increase linearly with field strength. For this reason it is more useful to measure chemical shifts as fractions, usually stated in *parts per million* (ppm). Secondly it is usually impractical to define chemical shifts with respect to the applied field, and so they are usually defined by the shift from some conventional reference system. Thirdly the induced fields depend on the relative orientation of the magnetic field and the molecular axes, and so chemical shift is a tensor, not a scalar [6, 12]. In spectra from solid powder samples [12] one observes the whole range of the tensor, and so very broad lines, but in liquids and solutions molecular tumbling causes rapid modulation of the chemical shift tensor. This averages the chemical shift interaction to its isotropic value.

### 1.3 Spin–spin coupling

When NMR spectra are acquired with better resolution, peaks split into groups called multiplets. Patterns in these splittings clearly indicate that they must come from some sort of coupling between spins. The most obvious explanation is direct coupling between pairs of magnetic dipoles, but it is easily seen that this cannot be the case. The dipole–dipole coupling strength is given by

$$D_{ij} \propto \frac{3 \cos^2 \theta_{ij} - 1}{r_{ij}^3} \quad (1.2)$$

where  $r_{ij}$  is the separation of nuclei  $i$  and  $j$  and  $\theta_{ij}$  is the angle between the internuclear vector and the main magnetic field. In solid samples the dipolar coupling is clearly visible [12], but in liquids and solutions the coupling is modulated by molecular tumbling and averages to its isotropic value, which is zero.

In fact the splittings arise from the the so-called J-coupling interaction, also called scalar coupling [5,6]. This additional coupling is related to the electron-nuclear hyperfine interaction. It is mediated by valence electrons, and thus only occurs between “nearby” spins; in particular it does not occur between nuclei in different molecules. Like dipolar coupling J-coupling is anisotropic, but unlike dipolar coupling it has a non-zero average (the isotropic value) which survives the molecular motion.

J-coupling has the form of a Heisenberg interaction, but in practice it is often truncated to an Ising form. For two coupled spins the total spin Hamiltonian is given by

$$\begin{aligned}\mathcal{H} &= \frac{1}{2}\omega_1\sigma_{1z} + \frac{1}{2}\omega_2\sigma_{2z} + \frac{1}{4}\omega_{J_{12}}\sigma_1 \cdot \sigma_2 \\ &\approx \frac{1}{2}\omega_1\sigma_{1z} + \frac{1}{2}\omega_2\sigma_{2z} + \frac{1}{4}\omega_{J_{12}}\sigma_{1z}\sigma_{2z}\end{aligned}\quad (1.3)$$

where all energies have been written in angular frequency units. Replacing the Heisenberg coupling by an Ising coupling corresponds to first-order perturbation theory, and is usually called the weak coupling approximation.

#### 1.4 The vector model and product operators

NMR spectroscopy appears quite different from conventional optical spectroscopy, as NMR experiments are essentially always in the coherent control regime. This is because it is trivial to make intense coherent RF fields and because NMR relaxation times are extremely long. For these reasons incoherent NMR spectroscopy is essentially unknown: all modern NMR spectroscopy is built round Rabi flopping and Ramsey fringes.

Simple NMR experiments are usually described using the *vector model*, which is based on the Bloch sphere [3,5,9]. A single isolated spin in a pure state  $|\psi\rangle$  can be described by a density matrix

$$|\psi\rangle\langle\psi| = \frac{1}{2}(\mathbf{1} + r_x\sigma_x + r_y\sigma_y + r_z\sigma_z) \quad (1.4)$$

and for a pure state  $r_x^2 + r_y^2 + r_z^2 = 1$  so  $\mathbf{r}$ , the nuclear spin vector, lies on the surface of the Bloch sphere. For a mixed state the situation is similar but the Bloch vector is not of unit length.

The behaviour of a single isolated spin is exactly described by its Bloch vector, and the behaviour of the Bloch vector is identical to that of a classical magnetisation vector. Thus the average behaviour of a single isolated spin can be described using the classical vector model. This is not true of coupled spin systems, where it is essential to use quantum mechanics.

The behaviour of coupled spin systems in NMR experiments is usually described using *product operators* [2,6,9–11]. These are very closely related to conventional angular momentum operators, but differ in normalisation and other conventions. While they can seem strange it is essential to get used to them! The state of a single spin is described as a combination of four one-spin operators:  $\frac{1}{2}E$ ,  $I_x$ ,  $I_y$  and  $I_z$ . (In NMR experiments the first spin is traditionally called  $I$ , while later spins are usually called  $S$ ,  $R$  and  $T$  in that order.) The last three operators are simply related to the conventional Pauli matrices by  $I_x = \frac{1}{2}\sigma_x$ , and so on, while  $\frac{1}{2}E = \mathbf{1}/2$  is the identity matrix normalised to have trace one (the maximally mixed state). In this notation nuclear spin Hamiltonians will be subtly different from their traditional forms: for a single spin  $\mathcal{H} = \omega_I I_z$ .

The initial state of an isolated nuclear spin at thermal equilibrium is given by the usual Boltzmann formula

$$\begin{aligned} \rho &= \exp(-\hbar\omega_I I_z/kT) / \text{tr} [\exp(-\hbar\omega_I I_z/kT)] \\ &\approx \frac{1}{2}E - \hbar\omega_I I_z/kT \end{aligned} \quad (1.5)$$

The first term (the maximally mixed state) is not affected by subsequent unitary evolutions and so is of little interest; for this reason it is usually dropped. Similarly the factors in front of the  $I_z$  term simply determine the size of the NMR signal, and are also usually neglected. Thus the thermal state of a single state is usually described as  $I_z$ .

Clearly this approach must be used with caution as  $I_z$  is not a proper density matrix: it corresponds to negative populations of some spin states! These apparent negative populations arise simply because the maximally mixed component has been neglected. The traditional NMR approach of concentrating on the traceless part of the density matrix is usually not a problem; in particular the evolution of an improper density matrix under a Hamiltonian can be calculated using the standard Liouville–von Neumann equation [2,4], as unitary evolutions are linear. For simple Hamiltonians the evolution can be calculated algebraically

$$I_x \xrightarrow{\omega t I_z} e^{-i\omega t I_z} I_x e^{i\omega t I_z} = I_x \cos \omega t + I_y \sin \omega t \quad (1.6)$$

and the product operator notation has been developed to enable this algebraic approach to be used as far as possible.

The success of this approach relies on the properties of commutators [6,9–11]. Consider an initial density matrix  $\rho(0) = A$  evolving under a Hamiltonian  $\mathcal{H} = bB$  for a time  $t$ . Suppose that  $[A, B] = iC$  and that  $[C, B] = -iA$ ; in this case the three operators  $A$ ,  $B$  and  $C$  form a triple, and in general

$$\rho(t) = A \cos bt - C \sin bt \quad (1.7)$$

which can be summarised as

$$A \xrightarrow{B} -C \xrightarrow{B} -A \xrightarrow{B} C \xrightarrow{B} A. \quad (1.8)$$

Clearly  $I_x$ ,  $I_z$  and  $-I_y$  form such a triple, but many analogous triples exist, allowing many quantum mechanical calculations to be performed using nothing more than elementary trigonometry and a table of commutators!

### 1.5 Experimental practicalities

Before proceeding to more sophisticated experiments it is useful to consider the elementary experimental phenomena of excitation, detection, and relaxation.

At thermal equilibrium the Bloch vector lies along the  $z$ -axis, and we must begin by exciting the spins. This can be achieved by a magnetic field of strength  $B_1$  which rotates around the  $z$ -axis at the Larmor frequency. The situation is most simply viewed in a rotating frame which also rotates around the  $z$ -axis at the Larmor frequency: thus the excitation field appears static, along the  $y$ -axis for example. The Bloch vector will precess around this excitation field at a rate  $\omega_1 = \gamma B_1$  towards the  $x$ -axis of the rotating frame. After a time  $t$  the Bloch vector has precessed through an angle  $\theta = \omega_1 t$ , and particularly important cases are the  $\pi/2$  and  $\pi$  pulses. The magnetic field is obtained by applying RF radiation, and we can choose the axis (in the rotating frame) about which the precession occurs by choosing the RF phase. Thus we can talk about, for example,  $x$  and  $y$  pulses [3].

NMR signal detection is best described using a classical view [8]. The ensemble average of the spins behaves like a classical magnetisation rotating at the Larmor frequency, and the NMR detector is a coil of wire wrapped around the sample. As the magnetisation cuts across the wires it induces an EMF in the coil which can be detected. This detection method corresponds to a weak ensemble measurement, rather than the hard projective measurements more usually considered in quantum systems. This fact, which can be ultimately traced back to the low energy of NMR transitions, has considerable significance for both conventional NMR experiments and for NMR quantum computing.

Another consequence of the low energy scale of NMR transitions is that spontaneous emission is essentially negligible, and only stimulated processes occur. Because of this NMR relaxation times can be very long (several seconds). Stimulated emission requires a magnetic field oscillating at the Larmor frequency, and modulation of the chemical shift and dipole–dipole Hamiltonians by molecular motion is the main source of relaxation for spin-half nuclei in liquids.

NMR relaxation of a single isolated spin is well described by two time constants:  $T_2$  (the transverse relaxation time) is the time scale of the loss of



$xy$ -magnetisation, that is the decoherence time, while  $T_1$  (the longitudinal relaxation time) is the time scale of recovery of the Boltzmann equilibrium population difference, and determines the repetition delay between experiments. For more complex spin systems the behaviour is broadly similar but more complex. Relaxation effects (especially short  $T_2$  times) can be a hindrance, but detailed studies of relaxation properties can provide useful information on molecular motions.

### 1.6 Spin echoes and two-spin systems

Spin echoes [3, 9, 13] play a central role in almost all NMR pulse sequences. In the one-spin case they are easily understood using the vector model. Start off with magnetisation along the  $x$ -axis and allow it to undergo free precession at the Larmor frequency  $\omega$  for a time  $t$ : the magnetisation will rotate towards the  $y$ -axis through an angle  $\omega t$ . Now apply a  $\pi_x$  pulse, giving a  $180^\circ$  rotation around the  $x$ -axis, so that the magnetisation appears to have rotated by  $-\omega t$ . Allow the magnetisation to precess for a further time  $t$ ; it will now return back to the  $x$ -axis whatever the value of  $\omega$ ! This behaviour can be easily calculated using product operators

$$\begin{aligned}
 I_x &\xrightarrow{\omega t I_z} I_x \cos \omega t + I_y \sin \omega t \\
 &\xrightarrow{\pi I_x} I_x \cos \omega t - I_y \sin \omega t \\
 &\xrightarrow{\omega t I_z} I_x \cos \omega t \cos \omega t + I_y \cos \omega t \sin \omega t - I_y \sin \omega t \cos \omega t + I_x \sin \omega t \sin \omega t \\
 &= I_x [\cos^2 \omega t + \sin^2 \omega t] = I_x
 \end{aligned} \tag{1.9}$$

to get exactly the same result.

The situation is similar but slightly more complex in two spin systems. These are described using 16 basic operators, formed by taking products of the four  $I$  spin and  $S$  spin operators and multiplying by two:

$$\begin{array}{cccc}
 \frac{1}{2}E & S_x & S_y & S_z \\
 I_x & 2I_x S_x & 2I_x S_y & 2I_x S_z \\
 I_y & 2I_y S_x & 2I_y S_y & 2I_y S_z \\
 I_z & 2I_z S_x & 2I_z S_y & 2I_z S_z
 \end{array} \tag{1.10}$$

The (weak coupling) Hamiltonian for a two spin system is then

$$\mathcal{H} = \omega_I I_z + \omega_S S_z + \pi J 2I_z S_z. \tag{1.11}$$

Product operators have the extremely useful property that all pairs of operators either commute or form triples, just like  $I_x$ ,  $I_y$  and  $I_z$ ; this means that the method of commutators, described in section (1.4) can also be used in two spin systems. For a table of the main commutators see Appendix A; a more complete list is available in [11].

Spin echoes can easily be performed in two-spin systems, but the result depends on whether the system is *heteronuclear* (the two spins are of different nuclear species, with very different Larmor frequencies) or *homonuclear* (the two spins are of the same nuclear species, with very similar Larmor frequencies). In a heteronuclear spin system only one spin (say  $I$ ) will be excited by the  $\pi$  pulse. In this case the  $I$  spin Zeeman interaction and the spin–spin coupling are refocused by the spin echo but the  $S$  spin Zeeman interaction is retained:

$$I_x + S_x \xrightarrow{\mathcal{H}} \xrightarrow{\pi I_x} \xrightarrow{\mathcal{H}} I_x + S_x \cos \omega_S t + S_y \sin \omega_S t. \quad (1.12)$$

In a homonuclear spin system, by contrast, both spins will normally be excited by the  $\pi$  pulse. In this case both Zeeman interactions are refocused but the spin–spin coupling is retained:

$$I_x + S_x \xrightarrow{\mathcal{H}} \xrightarrow{\pi(I_x + S_x)} \xrightarrow{\mathcal{H}} I_x \cos \pi J t + 2I_y S_z \sin \pi J t + S_x \cos \pi J t + 2I_z S_y \sin \pi J t. \quad (1.13)$$

It is of course possible to perform a “homonuclear” spin echo in a heteronuclear spin system, by simply applying separate  $\pi$  pulses to spins  $I$  and  $S$  at the same time. It is also possible to perform a “heteronuclear” spin echo in a homonuclear spin system by using low power *selective* pulses, which will excite one spin while leaving the other untouched. A high power pulse which excites all the spins of one nuclear species is usually called a *hard* pulse.

More complex pulse sequences can be built up by combining spin echoes and selective and hard pulses. This is a highly developed NMR technique which has led to a host of conventional NMR experiments with whimsical names such as COSY, NOESY and INEPT [6, 8, 11]. Using this approach one can create a pulse sequence whose total propagator corresponds to all sorts of unitary transformations—including quantum logic gates!

## 2 NMR and quantum logic gates

In this section I will describe how NMR techniques can be used to implement the basic gates required for quantum computation.

### 2.1 Introduction

Quantum logic gates [14] are simply unitary transformations which implement some desired logic operation. It has long been known by the NMR community that NMR techniques in principle provide a universal set of Hamiltonians, that is they can be used to implement *any* desired unitary evolution, including quantum logic gates. Building NMR quantum logic gates is very similar to designing conventional NMR pulse sequences, and

progress in this field has been very rapid. Furthermore many of the pulse sequences used to implement quantum logic are in fact very similar to common NMR pulse sequences, and it could be argued that many conventional NMR experiments are in fact quantum computations!

Although NMR techniques could be used to directly implement any desired quantum logic gate, this is not a particularly sensible approach. Instead it is usually more convenient to implement a *universal* set of quantum logic gates, and then obtain other gates by joining these basic gates together to form networks [14]. However one should be careful not to take this process too far. Theoreticians are often interested in implementing networks using the smallest possible set of basic resources, and it is known that in principle only *one* basic logic gate is required for quantum computation [15–18]. For experimentalists gates usually come in families, such that the ability to implement any one member of a family implies the ability to implement any other member of the family in much the same way, and it is more sensible to develop a fairly small set of simple but useful families of logic gates. For NMR quantum computing [19–22] the best set seems to be a set containing many (but not all) single qubit gates and the family of Ising coupling gates.

## 2.2 Single qubit gates

Single qubit gates correspond to rotations of a spin about some axis. The simplest gates are rotations about axes in the  $xy$ -plane, as these can be implemented using resonant RF pulses. The *flip angle* of the pulse (the angle through which the spin is rotated) depends on the length and the power of the RF pulse, while the *phase angle* of the pulse (and hence the azimuthal angle made by the rotation axis in the  $xy$ -plane) can be controlled by choosing the initial phase angle of the RF. Rotations about the  $z$ -axis can be implemented using periods of precession under the Zeeman Hamiltonian, while rotations around tilted axes can be achieved using off-resonance RF excitation. It is, however, usually simpler not to use these last two approaches: instead all single qubit gates are built out of rotations in the  $xy$ -plane.

A simple example is provided by the composite  $z$ -pulse [23], which implements a  $z$ -rotation using  $x$  and  $y$ -rotations,

$$\theta_z \equiv 90_{-x}\theta_y90_x \equiv 90_y\theta_x90_{-y} \quad (2.1)$$

where the pulse sequence has been written using NMR notation, with time running from left to right, rather than using operator notation, in which operators are applied sequentially from right to left. A similar approach can be used to implement tilted rotations, such as the Hadamard gate

$$H \equiv 180_z90_y \equiv 90_y180_x90_{-y}90_y \equiv 90_y180_x \quad (2.2)$$

Any desired single qubit gate can be built in this fashion.

Even this approach, however, is over complex, as there is a particularly simple method of implementing  $z$ -rotations. Rather than rotating the spin, it is simpler to rotate its reference frame. This can be achieved by passing  $z$ -rotations forwards or backwards through a pulse sequence

$$\psi_z \theta_\phi \equiv \theta_{\phi-\psi} \psi_z \quad (2.3)$$

and altering pulse phase to reflect the new reference frame. This technique, often called *abstract reference frames* [22, 24] has the advantage that  $z$ -rotations can be implemented without using any time or resources! Many modern implementations of NMR quantum logic gates use only rotations in the  $xy$ -plane and changes in reference frames to implement all single qubit gates.

### 2.3 Two qubit gates

In addition to single qubit gates a design for a quantum computer must include at least one non-trivial two qubit gate. The most commonly discussed two qubit gate is the controlled-NOT gate, but this is not the most natural two qubit gate for NMR quantum computing. A controlled-NOT gate can be replaced by a pair of Hadamard gates and a controlled-phase-shift gate [22]

The diagram shows two equivalent quantum circuits for a two-qubit gate. On the left, a controlled-NOT gate is represented by a vertical line with a solid dot on the top wire (control) and a circle with a plus sign on the bottom wire (target). On the right, a controlled-phase-shift gate is shown with a vertical line and a solid dot on the top wire, and a solid dot on the bottom wire. This controlled-phase-shift gate is flanked by Hadamard (H) gates on both the top and bottom wires. The two circuits are separated by an equivalence symbol (≡). The equation number (2.4) is to the right of the diagram.

where the controlled-phase-shift gate acts to negate the state  $|11\rangle$  while leaving other states unchanged. Note that this gate acts symmetrically on the two qubits; it does not have control and target bits. The asymmetry in the controlled-NOT gate arises from the asymmetry in the placement of the Hadamard gates.

The controlled-phase-shift gate is itself equivalent (up to single qubit  $z$ -rotations, which can be adsorbed into abstract reference frames) to the Ising coupling gate

$$e^{i(\phi/2)2I_z S_z} = \begin{pmatrix} e^{-i\phi/4} & 0 & 0 & 0 \\ 0 & e^{-i\phi/4} & 0 & 0 \\ 0 & 0 & e^{i\phi/4} & 0 \\ 0 & 0 & 0 & e^{i\phi/4} \end{pmatrix} \quad (2.5)$$

where the case  $\phi = \pi$  forms the basis of the controlled-NOT gate. This “gate” is nothing more than a period of evolution under the Ising coupling Hamiltonian, which can be achieved using a homonuclear spin echo.



The effect of a  $180^\circ$  pulse on a spin system is, in effect, to negate the sign of the Zeeman and spin coupling terms involving that spin; simultaneous  $180^\circ$  pulses on two spins will negate the coupling between these spins *twice*, thus leaving it unchanged. This gives a simple way of analysing the effect of spin echo sequences. Each interaction term in the Hamiltonian begins the sequence with a relative strength of +1, and each  $180^\circ$  pulse on a spin negates every term involving that spin. The effect of a spin echo sequence on a Zeeman interaction can be determined by writing down a vector of +1 and  $-1$  terms, and then summing along the components of the vector. The effect on a J-coupling between two spins can be determined by multiplying corresponding elements in the two vectors and then summing them, that is by taking the dot product of two vectors. A spin echo sequence refocuses Zeeman interactions if vectors sum to zero, and refocuses J-couplings if vectors are orthogonal.

This approach can be used to analyse existing spin echo schemes, but it can also be used to design new ones: a set of vectors with the desired properties is constructed, and then a pulse sequence is designed by applying a  $180^\circ$  pulse to a spin every time to vector changes sign. Suitable vectors can easily be obtained by taking rows from Hadamard matrices to obtain efficient refocusing schemes. For example the four by four Hadamard matrix

$$H_4 = \begin{pmatrix} 1 & 1 & 1 & 1 \\ 1 & -1 & 1 & -1 \\ 1 & 1 & -1 & -1 \\ 1 & -1 & -1 & 1 \end{pmatrix} \quad (2.8)$$

can be used to derive an efficient scheme for four spins:

(2.9)

The gain is not huge for small spin systems, but becomes dramatic in large systems: Hadamard based schemes [25, 26] require only  $O(N^2)$  pulses to refocus all couplings in an  $N$ -spin system.

When building NMR quantum computers with more than three spins, it may be easier to use “linear” spin systems, in which each spin is only coupled to its immediate neighbours, or other partially coupled systems. A

linear spin system can be used to implement any logic gate by using SWAP gates to move qubits around the system; this imposes an overhead but this is only linear in the number of spins in the system.

Whatever refocusing scheme is adopted, large NMR quantum computers will require the use of selective pulses in homonuclear spin systems (it is not possible to build a large fully heteronuclear spin system as there are not enough spin half nuclei). One can selectively excite a single nuclear spin in a homonuclear spin system, while leaving the others untouched, by using long low-power pulses. The excitation bandwidth of a pulse is given approximately by the inverse of its duration, and selective pulses are usually shaped, that is amplitude and phase modulated, to give them better excitation profiles. Many complicated shaped pulses have been designed [3], which rely on sophisticated NMR hardware for their implementation, but for NMR quantum computing some of the simplest types (Gaussian and Hermite pulses) seem to be best.

An alternative scheme is to implement selective pulses using sequences of hard pulses and delays [22,27]. During delay periods spins will evolve under the background Hamiltonian, which is dominated by Zeeman interactions, and so different spins will experience different  $z$ -rotations. Sandwiching these  $z$ -rotations between  $90_{\pm y}^{\circ}$  pulses converts the varying  $z$ -rotations into corresponding  $x$ -rotations, in effect implementing selective pulses [22,27].

The opposite approach, using selective pulses to implement two qubit gates has also been demonstrated [28]. In this case it is necessary to use extremely long low power pulses which excite one line in a multiplet while leaving other lines untouched. This provides a simple method for implementing multiply-controlled-NOT gates, such as TOFFOLI gates, but it seems unlikely that this approach will be generally useful.

Finally when considering quantum logic gates it is essential to remember that writing down a Hamiltonian is not the same as implementing a gate! Real experimental gates are vulnerable to both random and systematic errors, and the effects of these must be considered. This point will be treated in some depth in lecture 4.

## 2.5 Non-unitary gates

Although quantum computations are usually thought of as a sequence of unitary gates, non-unitary gates also play a key role in quantum information processing. The most obvious examples are projective measurements and the initialisation of qubits, but as discussed in lecture 3 these processes are difficult or impossible to implement in NMR systems. It is, however, possible to implement other non-unitary gates, and these are extremely important.

In general a non-unitary gate can be implemented by using a unitary gate to entangle the system with some aspect of the environment and then tracing out this environmental information. The two basic non-unitary gates

in NMR use the position of spins in the spatial ensemble or the time at which an experiment was performed as the environmental label.

In modern NMR experiments the most common non-unitary is a *gradient pulse* [11]. For a short time the magnetic field is made highly inhomogeneous, so that the Larmor frequency varies strongly over the sample. This causes off-diagonal terms in the density matrix to dephase over the sample, and thus to disappear when the final NMR signal is detected. The situation is not, however, as simple as is sometimes described, as some off-diagonal terms (known in NMR notation as homonuclear zero quantum coherences) will survive the dephasing: these dephasing free subspaces are analogous to the decoherence free subspaces [29, 30] suggested for building robust quantum bits.

Gradient pulses are most commonly used as *crush* pulses; these convert visible NMR terms, such as  $I_x$  and  $I_y$ , into the maximally mixed state, in effect destroying them. Crush pulses are automatically applied to all the spins in a spin system, but some spins may be unaffected because of their initial state. The action of projecting spins onto the  $z$ -axis can be used, for example, to render error terms invisible or to change the relative polarisations of two spins

$$I_z + S_z \xrightarrow{\pi/3 I_y} \frac{1}{2} I_z + \frac{\sqrt{3}}{2} I_x + S_z \xrightarrow{\text{crush}} \frac{1}{2} I_z + S_z. \quad (2.10)$$

It is important to realise that crush pulses are only apparently non-unitary: the dephasing retains its spatial label and can be refocused. In particular crush pulses will interact with spin echoes; this can be a problem in sequences with many gradients, as it can lead to accidental refocusing of supposedly crushed terms. One solution to this is to use gradients along different spatial axes, and well equipped spectrometers will have three orthogonal gradients ( $x$ ,  $y$ , and  $z$ ); similar effects can be achieved by dephasing the spin system with inhomogeneous RF fields. More usefully the combination of gradients and spin echoes gives a route to selective crush pulses

$$I_x + S_x \xrightarrow{\text{crush}} \xrightarrow{\pi I_y} \xrightarrow{\text{crush}} I_x \quad (2.11)$$

which only affect one spin in a mult-spin system.

If necessary it is possible to obtain a true non-unitary gate by destroying the spatial label. This can be achieved by spatial diffusion of the spin system within the ensemble, either during the crush pulse or between two crush pulses. This approach is sometimes called *engineered decoherence* [30].

A second route to non-unitary processes in NMR is to use temporal rather than spatial labels. This can be achieved by repeating the same basic pulse sequence several times, making subtle changes each time, and then taking linear combinations of the resulting NMR signals, so that some terms add together while other terms cancel out. The simplest approach



is to alter the relative phase of pulses, in which case it is known as phase cycling [11]. Phase cycling techniques were very widely used in conventional NMR experiments, but in recent years have been largely superseded by gradients. They have, however, found new applications in NMR quantum computing where they form the basis of the popular *temporal averaging* schemes for initialisation.

### 3 NMR quantum computers

In this section I will describe how NMR quantum computers overcome the difficulties inherent in NMR to perform initialisation and readout. In particular I will describe the use of pseudo-pure states, and the implications of this approach for the efficiency of NMR quantum computing. Finally I will briefly describe the implementation of a quantum cloning on an NMR quantum computer.

#### 3.1 Introduction

From the description given in the previous lecture it would seem that NMR was very well suited to the task of implementing quantum computers. There are, however, substantial problems with NMR as a quantum information processing technology [31], which stem from difficulties in initialising nuclear spin states and in reading out the final result.

Conventional designs for quantum computers [32] use single quantum systems which start in a well defined initial state. While details may vary, this initialisation is usually achieved by cooling the system to its thermodynamic ground state. NMR quantum computers [19–22], by contrast, use an ensemble of molecules which start in a hot thermal state, because even for the very large fields used in NMR spectrometers the Zeeman energy gap between the two spin states is tiny compared to  $kT$ . One could imagine lowering the temperature so that NMR enters the low temperature regime, but this would require cooling the system well below 1 mK; although this is possible the sample would certainly not remain in the liquid state. A potentially better approach is to use non-Boltzmann initial populations, as discussed in lecture 5. Almost all implementation of NMR quantum computing, however, simply sidestep this issue by forming a “pseudo-pure” initial state from the thermal state as discussed below.

Similar problems also occur with methods for reading out the final result. Conventional quantum computers achieve read out by hard (projective) measurements, while NMR quantum computers use weak ensemble measurements, which do not project the spin system. This can be seen by realising that a conventional NMR measurement (observation of the free induction decay) can be described quantum mechanically as the continuous and simultaneous observation of two non-commuting observables,  $I_x$  and  $I_y$ .

This is also the approach used for readout in NMR quantum computers, and a simple example is shown in Fig. 1



**Fig. 1.** NMR spectrum showing readout from a two qubit NMR quantum computer based on the two  $^1\text{H}$  nuclei in cytosine [33]; the negative intensity on the left hand multiplet indicates that the corresponding qubit was in state  $|1\rangle$ , while the positive intensity indicates that this qubit was in state  $|0\rangle$ .

These weak measurements might seem more powerful than conventional projective measurements, but in fact they are less useful for two reasons. Firstly the use of projective measurements permits the use of measurements followed by classical control; by contrast NMR quantum computers can only use quantum control methods. More importantly, projective measurements provide an excellent initialisation method: just measure a bit, and then flip it if it has the wrong value! In particular reinitialisation of ancilla qubits through the use of projective measurements plays a key role in quantum error-correction protocols [34].

### 3.2 Pseudo-pure states

The history of NMR quantum computing in effect begins with the realisation by David Cory and coworkers [19,20] that while it is difficult to form a pure initial state it is easy to form states whose behavior is almost identical. Such states, known as pseudo-pure states or effective pure states, take the form

$$\rho = (1 - \epsilon)\frac{\mathbf{1}}{2^n} + \epsilon|0\rangle\langle 0|, \quad (3.1)$$

that is mixtures of the maximally mixed state and the desired initial state with purity  $\epsilon$ . As the maximally mixed state does not evolve under any unitary transformation it will be unchanged by any quantum computation. Furthermore, all NMR observables are traceless [11], and so the maximally mixed state gives no observable signal. For this reason the presence of the maximally mixed state can, in effect, be ignored, and the behaviour of a pseudo-pure state is identical to that of the corresponding pure state up to a scaling factor [22].

As an example, consider a homonuclear spin system of two spin-half nuclei. This has four energy levels with nearly equal populations, but the population of the lowest level will of course be slightly greater than that of any other level. This excess population provides the basis of pseudo-pure

state formation, but the state as described is *not* a pseudo-pure state, as the upper levels do not all have the same population. Suppose, however, that some non-unitary process is applied which equalises the populations of the upper levels, while leaving the lowest level untouched: the result will be the desired pseudo-pure state [35]. To understand the behaviour of this state imagine going through the ensemble, taking out molecules in groups of four (one in each spin state) and placing them in a box; eventually there will be a large box containing equal populations of all four spin states and a small excess of the  $|00\rangle$  spin state remaining. The NMR signals from the molecules in the box will all cancel out, leaving only the signal from the small excess: the pseudo-pure state.

Pseudo-pure states can also be described more accurately using the product operator approach [22, 36]. The Boltzmann equilibrium state of a homonuclear two-spin system is approximately

$$\rho_B \approx \frac{1}{2}E + \delta(I_z + S_z) = \frac{1}{2}E + \delta\{1, 0, 0, -1\} \quad (3.2)$$

where the braces indicate a *diagonal* density matrix described by listing its diagonal elements. The ideal pure ground state takes the form

$$\rho_0 = \frac{1}{2}(\frac{1}{2}E + I_z + S_z + 2I_zS_z) = \{1, 0, 0, 0\} \quad (3.3)$$

and so forming a pseudo-pure ground state will require the creation of a  $2I_zS_z$  component and the rescaling of other terms so that each term is present in the correct *relative* quantity. Clearly this will require a combination of unitary and non-unitary processes, and three main approaches have been described.

The original *spatial averaging* method of Cory *et al.* [19, 20] for creating a pseudo-pure state in a two spin system used a sequence of (unitary) pulses and delays combined with (non-unitary) crush gradients. The method is easily understood using product operators:

$$\begin{aligned} I_z + S_z &\xrightarrow{60^\circ S_x} I_z + \frac{1}{2}S_z - \frac{\sqrt{3}}{2}S_y \\ &\xrightarrow{\text{crush}} I_z + \frac{1}{2}S_z \\ &\xrightarrow{45^\circ I_x} \frac{1}{\sqrt{2}}I_z - \frac{1}{\sqrt{2}}I_y + \frac{1}{2}S_z \\ &\xrightarrow{\text{Ising}} \frac{1}{\sqrt{2}}I_z + \frac{1}{\sqrt{2}}2I_xS_z + \frac{1}{2}S_z \\ &\xrightarrow{45^\circ I_x} \frac{1}{2}I_z - \frac{1}{2}I_x + \frac{1}{2}2I_xS_z + \frac{1}{2}S_z + \frac{1}{2}2I_zS_z \\ &\xrightarrow{\text{crush}} \frac{1}{2}(I_z + S_z + 2I_zS_z). \end{aligned} \quad (3.4)$$

An widely used alternative, *temporal averaging* [37], uses permutation operations to create different initial states

$$I_z + S_z \xrightarrow{P_0} \{1, 0, 0, -1\}$$

$$\begin{aligned} I_z + S_z &\xrightarrow{F_1} \{1, 0, -1, 0\} \\ I_z + S_z &\xrightarrow{F_2} \{1, -1, 0, 0\} \end{aligned} \quad (3.5)$$

and averaging over these three separate experiments gives an effective pure state

$$\rho_{TA} = \{1, -\frac{1}{3}, -\frac{1}{3}, -\frac{1}{3}\}. \quad (3.6)$$

This method has the advantage of being easy to understand and to generalise to larger spin system, but the disadvantage that several different experiments are required. Indeed if the most obvious scheme, exhaustive permutation, is implemented a very large number of experiments may be required; fortunately less profligate partial averaging schemes are known [37].

Finally the *logical labelling* approach of Gershenfeld and Chuang [21] provides a conceptually elegant method for using naturally occurring subsets of levels in larger systems as pseudo-pure states. As an example consider a three spin system

$$I_z + S_z + R_z = \frac{1}{2}\{3, 1, 1, -1, 1, -1, -1, -3\} \quad (3.7)$$

and pick out the subset of four levels with relative populations 3,  $-1$ ,  $-1$  and  $-1$ , that is the levels  $|000\rangle$ ,  $|011\rangle$ ,  $|101\rangle$  and  $|110\rangle$ . The most direct approach is just to work in this subset, but it usually more convenient to permute populations so that the levels  $|000\rangle$ ,  $|001\rangle$ ,  $|010\rangle$  and  $|011\rangle$  can be used; this makes implementing logic gates much simpler.

Perhaps the most practical general scheme for preparing pseudo-pure states is based on the use of ‘‘cat’’ states [24], which are states of the form

$$\psi_{\pm}^n = |00\dots 0\rangle \pm |11\dots 1\rangle \quad (3.8)$$

for an  $n$ -qubit system, that is equally weighted superpositions of the state in which all  $n$  qubits are in  $|0\rangle$  and the state in which all qubits are in  $|1\rangle$ . It is easy both to reach the state  $\psi_{\pm}^n$  starting from the ground state  $|00\dots 0\rangle$ , and to convert the cat state back to the ground state. This may not seem useful, but it is relatively simple to design non-unitary filter schemes, using either spatial or temporal averaging, which convert all states except  $\psi_{\pm}^n$  into the maximally mixed state. The Boltzmann equilibrium state can thus be converted to a mixed state including a component of  $\psi_{\pm}^n$ , and after filtration the  $\psi_{\pm}^n$  state can be converted back to  $|00\dots 0\rangle$ . The filter schemes, however, also retain any  $\psi_{\pm}^n$  component, and this is converted into  $|10\dots 0\rangle$ . The overall effect is to produce the state  $I_z \otimes |0\dots 0\rangle\langle 0\dots 0|$ , that is a pseudo-pure state of  $n - 1$  qubits.

### 3.3 Efficiency of NMR quantum computing

The discussion so far has neglected any consideration of the level of purity which can be achieved in a pseudo-pure state; this is most simply quantified

by the value of  $\epsilon$  in Eq. 3.1. At one level this is unimportant, as  $\epsilon$  simply determines the intensity of the observed NMR signal, but if  $\epsilon$  becomes too small this will render the NMR signal undetectable. Unfortunately for NMR quantum computing, the value of  $\epsilon$  drops exponentially with the number of qubits in the system: for every additional qubit the available signal intensity approximately halves [38].

This effect is not, as is sometimes suggested, a peculiar fault of NMR quantum computers: rather it is a simple consequence of working in the high temperature limit. It does, however, mean that pseudo-pure states extracted from thermal equilibrium systems cannot provide a route to scalable NMR quantum computers.

More controversially some authors have implied that NMR quantum computers are not quantum computers at all! How this claim is assessed depends on exactly what is meant by “NMR quantum computers”, and even what is meant by “quantum computing”. However, while there is substantial room for philosophical debates, the underlying science is now relatively clear. On the one hand it is known that high temperature pseudo-pure states cannot lead to provably entangled states [39], and that such systems cannot give efficient implementations of Shor’s quantum factoring algorithm [40]. On the other hand it so far proved impossible to develop a purely classical model of pseudo-pure state NMR quantum computing: while it is possible to describe the state of an NMR device at any point in a computation using a classical model, it appears to be impossible to develop a classical model of the transitions between these states [41].

It is also vital to remember that these arguments apply only to NMR quantum computers built using pseudo-pure states, and that there are other types of NMR quantum computing. For example some quantum algorithms only require one pure qubit: the other qubits can be in maximally mixed states [42]. Indeed, even the single “pure” qubit need not be pure: a pseudo-pure state will suffice. This type of NMR quantum computing is clearly scalable, although it can only be used for a limited range of algorithms. An alternative approach is to use a scheme described by Schulman and Vazirani, which allows a small number of nearly pure qubits to be distilled from a large number of impure qubits using only unitary operations [43]. This scheme needs  $O(\epsilon^{-2})$  impure spins for each pure spin extracted: this is a constant multiplicative overhead, and so has no scaling problem. Thus high temperature states, such as those used in NMR, do allow true quantum computing! Unfortunately the overhead for NMR systems of about  $10^{10}$  means that this method has only theoretical interest.

### 3.4 NMR quantum cloning

Finally I will end this lecture by briefly describing an NMR implementation of approximate quantum cloning [44]. This experiment is complicated

enough to be interesting, but simple enough that the basic ideas can be described in a fairly straightforward manner.

The no-cloning theorem, which states that an unknown quantum state cannot be exactly copied [45], is one of the oldest results in quantum information theory. Approximate quantum cloning is, however, possible, and a range of different schemes have been described. If one qubit is converted into two *identical* copies, such that the fidelity of the copies is independent of the initial state, then the maximum fidelity that can be achieved is  $\frac{5}{6}$ , and an explicit quantum circuit which achieves this is known [46]. If a state  $|\psi\rangle$  is cloned, the two copies take the form

$$\frac{5}{6}|\psi\rangle\langle\psi| + \frac{1}{6}|\psi^\perp\rangle\langle\psi^\perp| = \frac{2}{3}|\psi\rangle\langle\psi| + \frac{1}{3}(\mathbf{1}/2). \quad (3.9)$$

This circuit can also be used to clone a mixed state,  $\rho$  producing even more mixed clones of the form

$$\frac{2}{3}\rho + \frac{1}{3}(\mathbf{1}/2). \quad (3.10)$$

In the language of vectors on Bloch spheres, the two clones have Bloch vectors parallel to the original Bloch vector, but with only  $\frac{2}{3}$  the length [44].

The cloning circuit comprises two stages: *preparation*, which prepares two qubits into an initial “blank paper” state, suitable for receiving a copy, and *copying*, in which the initial qubit is copied onto these qubits. As the preparation stage simply prepares two blank qubits, and is independent of the state of the unknown qubit, the preparation stage can be replaced by any other transformation which has the same effect, and the NMR implementation, which is shown in Fig. 2 does indeed use a modified preparation stage. The copying stage, however, must implement the correct unitary transformation, and the implementation used the conventional copying circuit.

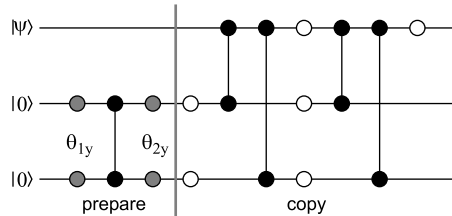


**Fig. 2.** A modified version of the approximate quantum cloning network: the new version is simpler to implement on the NMR system used. Filled circles connected by control lines indicate controlled phase shift gates, empty circles indicate single qubit Hadamard gates, while grey circles indicate other single qubit rotations. The two rotation angles in the preparation stage are  $\theta_1 = \arcsin(1/\sqrt{3}) \approx 35^\circ$  and  $\theta_2 = \pi/12 = 15^\circ$ .

The cloning circuit was implemented on a three-qubit NMR quantum computer based on the molecule based on the single  $^{31}\text{P}$  nucleus ( $P$ ) and the two  $^1\text{H}$  nuclei ( $A$  and  $B$ ) in E-(2-chloroethenyl)phosphonic acid (Fig. 3) dissolved in  $\text{D}_2\text{O}$ . The NMR pulse sequence used is shown in Fig. 4. This

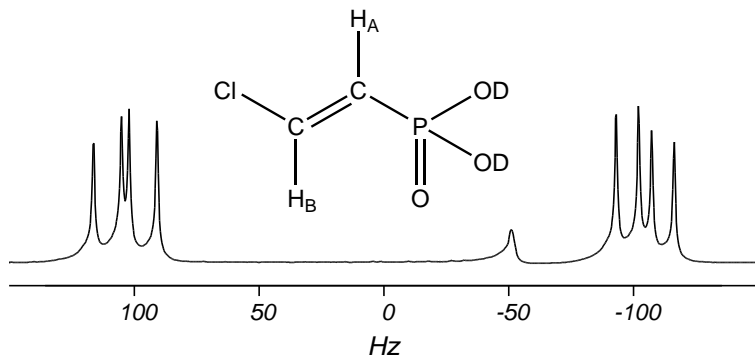


**Fig. 3.** The three qubit system provided by E-(2-chloroethenyl)phosphonic acid dissolved in  $\text{D}_2\text{O}$  and its  $^1\text{H}$  NMR spectrum. Following standard NMR conventions the spectrum has been plotted with frequencies measured as offsets from the reference RF frequency, and with frequency increasing from right to left. The broad peak near  $-50$  Hz can be ignored.

comprises two main sections: an initial purification sequence (a), used to generate an initial pseudo-pure state corresponding to  $P_z \otimes |0_A 0_B\rangle\langle 0_A 0_B|$ , and a preparation and cloning sequence (b), which implements the circuit shown in Fig. 2, cloning the state of  $P$  onto  $A$  and  $B$ . Both of these are built around the “echo” sequence (c), which implements the coupling element of the  $PA$  and  $PB$  controlled phase shifts by evolution of the spin system under the weak coupling Hamiltonian with undesirable Zeeman evolutions refocused by spin echoes. This requires selective  $90^\circ$  pulses, which are built out of hard pulses and delays as described in my second lecture. For further details see the original paper [44].

The results of the cloning circuit can be observed by detecting the NMR signal from the two  $^1\text{H}$  nuclei,  $A$  and  $B$ . The ideal spectrum should have equal intensities on the two outer lines of each multiplet, and no signal on the two central lines. Errors are seen in the experimental spectra, but the overall behaviour is clearly observed: Fig. 5 shows the result of cloning the state  $P_x$ . Results of similar quality are obtained when cloning other initial states [44].

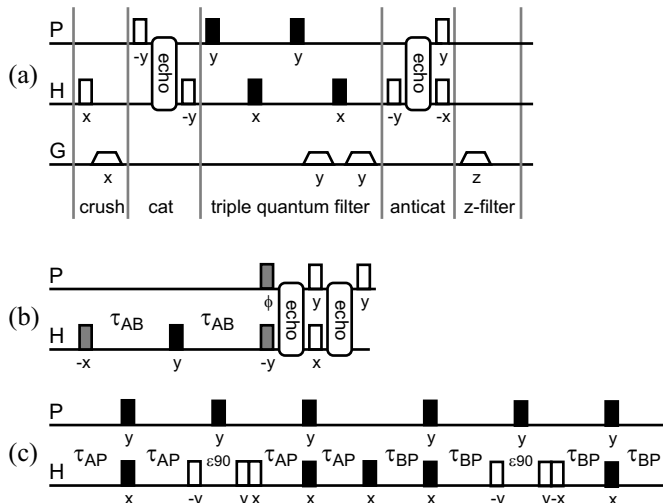


**Fig. 4.** The NMR pulse sequences used to implement quantum cloning. White and black boxes are  $90^\circ$  and  $180^\circ$  pulses, while grey boxes are pulses with other flip angles; pulse phases and gradient directions are shown below each pulse. All RF pulses are hard, with  $^1\text{H}$  frequency selection achieved using “jump and return” methods.

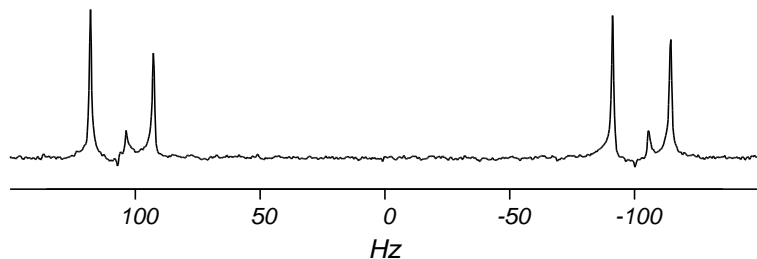


**Fig. 5.** The experimental result from cloning the initial state  $P_x$ ; the receiver phase was set using a separate experiment so that  $x$ -magnetization appears as positive absorption mode lines.

#### 4 Robust logic gates

In this section I will describe how techniques adapted from conventional NMR experiments can be used to develop robust logic gates for NMR quantum computers. Although developed and described within the context of NMR, these robust gates could be used in other implementations of quantum computing.



#### 4.1 Introduction

Quantum computers implement logic gates as periods of evolution under Hamiltonians which can be external (*e.g.*, RF pulses) or internal (*e.g.*, Ising couplings). Computation requires extremely accurate logic gates, and thus extremely accurate control of evolution rates. Naive estimates suggest that it may be difficult or impossible to control Hamiltonians with sufficient accuracy, but fortunately robust logic gates can be designed to tolerate small errors in these rates.

The approach described here is based on the NMR concept of *composite rotations* [3, 9, 47, 48], which have long been used to reduce the impact of systematic errors on conventional NMR experiments, but the basic idea is general and can be applied in many other fields. As usual it is not necessary to design robust versions of every conceivable logic gate: it suffices to develop a complete set of one and two qubit gates.

When considering the accuracy of logic gates it is necessary to measure the fidelity of the actual operation  $V$  in comparison with the desired operation  $U$ , and an obvious measure is provided by the propagator fidelity [49]

$$\mathcal{F} = \frac{|\text{tr}(VU^\dagger)|}{\text{tr}(UU^\dagger)} \quad (4.1)$$

where it is necessary to take the absolute value of the numerator to deal with (irrelevant) differences in global phases. The propagator fidelity works for any unitary operation, although it can be over complicated in practice and alternative measures have been suggested.

#### 4.2 Composite rotations

The use of composite rotations to reduce the effects of systematic errors in conventional NMR experiments relies on the fact that any state of a single isolated qubit can be mapped to a point on the Bloch sphere, and any unitary operation on a single isolated qubit corresponds to a rotation on the Bloch sphere. The result of applying any series of rotations (a composite rotation) is itself a rotation, and so there are many apparently equivalent ways of performing a desired rotation. These different methods may, however, show different sensitivity to errors: composite rotations can be designed to be much less error prone than simple rotations!

A rotation can go wrong in two basic ways: the rotation angle can be wrong or the rotation axis can be wrong. In an NMR experiment (viewed in the rotating frame) ideal RF pulses cause rotation of a spin through an angle  $\theta = \omega_1 t$  around an axis in the  $xy$ -plane. So called *pulse length errors* occur when the pulse power  $\omega_1$  is incorrect, so that the flip angle  $\theta$  is systematically wrong by some fraction. This can be due to experimenter carelessness, but more usually arises from the inhomogeneity in the RF field

over a macroscopic sample. The second type of error, *off-resonance effects* (Fig. 6), occur when the excitation frequency doesn't match the transition

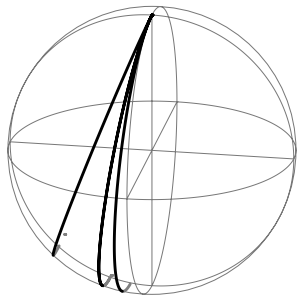


**Fig. 6.** Effect of applying an off-resonance  $180^\circ$  pulse to a spin with initial state  $I_z$ ; the spin rotates around a tilted axis. Trajectories are shown for small, medium and large off-resonance effects.

frequency, so that the Hamiltonian is the sum of RF and off-resonance terms. This results in rotations around a tilted axis, and the rotation angle is also increased.

The first composite rotation [47] was designed to compensate for pulse length errors in an inversion pulse, that is a pulse which takes the state  $I_z$  to  $-I_z$ . This can be achieved by, for example, a simple  $180_y^\circ$  pulse, but this is quite sensitive to pulse length errors. The composite rotation  $90_x^\circ 180_y^\circ 90_x^\circ$  has the same effect in the absence of errors, but will also partly compensate for pulse length errors. This is shown in Fig. 7 which plots the inversion efficiency of the simple and composite  $180^\circ$  pulses as a function of the fractional pulse length error  $g$ . (The inversion efficiency of an inversion pulse measures the component of the final spin state along  $-I_z$  after the pulse is applied to an initial state of  $I_z$ .)

Composite pulses of this kind are very widely used within conventional NMR, and many different pulses have been developed [48], but most of them are not directly applicable to quantum computing [50]. This is because conventional NMR pulse sequences are designed to perform specific motions on the Bloch sphere (such as inversion), in which case the initial and final spin states are known, while for quantum computing it is necessary to use general rotations, which are accurate whatever the initial state of the system. Perhaps surprisingly composite pulses are known which have the desired property, of performing accurate rotations whatever the initial spin state.

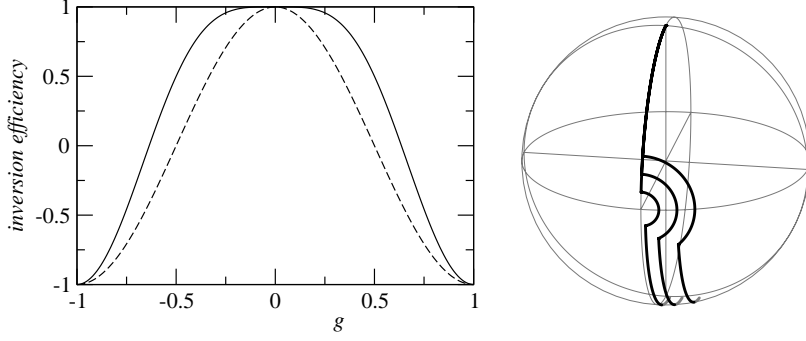


**Fig. 7.** The inversion efficiency of a simple  $180^\circ$  pulse (dashed line) and of the composite pulse  $90_x^\circ 180_y^\circ 90_x^\circ$  (solid line) as a function of the fractional pulse length error  $g$ . The way in which the composite pulse works can be understood by examining trajectories on the Bloch sphere, which are shown on the right for three values of  $g$ .

### 4.3 Quaternions and single qubit gates

Quaternions provide a simple and powerful way of describing rotations (single qubit gates), as they can be easily formed, combined, and compared. The quaternion corresponding to a  $\theta$  rotation around an axis at an azimuthal angle  $\phi$  in the  $xy$ -plane is given by

$$\mathbf{q}_{\theta\phi} = \{s, \mathbf{v}\} = \{\cos(\theta/2), \sin(\theta/2)(\cos(\phi), \sin(\phi), 0)\} \quad (4.2)$$

where  $s$  is a scalar depending on the rotation angle, and  $\mathbf{v}$  is a vector whose length depends on the rotation angle and which lies parallel to the rotation axis. The result of applying two rotations is given by the quaternion product

$$\mathbf{q}_1 * \mathbf{q}_2 = \{s_1 \cdot s_2 - \mathbf{v}_1 \cdot \mathbf{v}_2, s_1 \mathbf{v}_2 + s_2 \mathbf{v}_1 + \mathbf{v}_1 \wedge \mathbf{v}_2\} \quad (4.3)$$

and two quaternions can be compared using the quaternion fidelity

$$\mathcal{F}(\mathbf{q}_1, \mathbf{q}_2) = |\mathbf{q}_1 \cdot \mathbf{q}_2| = |s_1 \cdot s_2 + \mathbf{v}_1 \cdot \mathbf{v}_2|. \quad (4.4)$$

As a simple example consider a NOT gate, that is a  $180_x^\circ$  rotation. The quaternion for an ideal rotation is

$$\mathbf{q}_0 = \{0, (1, 0, 0)\} \quad (4.5)$$

while the quaternion representing this rotation in the presence of a fractional pulse length error  $g$  is

$$\mathbf{q}_1 = \{\cos[(1+g)\pi/2], (\sin[(1+g)\pi/2], 0, 0)\} \quad (4.6)$$

and so the quaternion fidelity is

$$\mathcal{F}_1 = |\sin((1+g)\pi/2)| = |\cos(g\pi/2)| \approx 1 - \frac{\pi^2 g^2}{8} \quad (4.7)$$

As an alternative consider the conventional composite pulse sequence for a  $180_x^\circ$  rotation,  $90_y^\circ 180_x^\circ 90_y^\circ$ , which has the quaternion form

$$\mathbf{q}_2 = \{\sin^2[g\pi/2], (\cos[g\pi/2], -\sin[g\pi/2], 0)\} \quad (4.8)$$

and gives exactly the same fidelity,  $\mathcal{F}_2 = |\cos(g\pi/2)| = \mathcal{F}_1$ . This confirms that the conventional sequence does not actually correct for errors when considered as a general rotation: the good behaviour for certain initial states is obtained at the cost of poor behaviour for other initial states.

An example of a NOT gate which does give genuine improvement [51,52] is provided by the sequence  $90_0^\circ 180_\phi^\circ 360_{3\phi}^\circ 180_\phi^\circ 90_0^\circ$ , with  $\phi = \arccos(-1/4)$ . The quaternion for this composite rotation in the presence of errors is complicated, but its fidelity is given by

$$\mathcal{F}_3 \approx 1 - \frac{5\pi^6 g^6}{1024} \quad (4.9)$$

showing that the second and fourth order error terms are completely cancelled. This BB1 sequence was originally developed by Wimperis for conventional NMR experiments [51], and later rederived using quaternions in the context of NMR quantum computing [52]. As shown in Fig. 8 the BB1 gate outperforms a naive NOT gate for all pulse length errors  $g$ , especially for errors in the range  $\pm 25\%$ . Its behaviour is essentially perfect for errors of less than 1%.

Similar gates can be developed to tackle off-resonance effects. Intriguingly the sequence  $90_x^\circ 180_y^\circ 90_x^\circ$  provides some compensation for off-resonance effects as long as the pulse length is correct, but as before this compensation only occurs for inversion, and so the composite pulse is not suitable for quantum computing. However suitable composite rotations are known: an early result by Tycko [53] has been refined and extended [52,54]: a simple  $\theta_x$  rotation should be replaced by the CORPSE sequence of three rotations along  $x$ ,  $-x$  and  $x$  with

$$\begin{aligned} \theta_1 &= 2\pi + \frac{\theta}{2} - \arcsin\left(\frac{\sin(\theta/2)}{2}\right) \\ \theta_2 &= 2\pi - 2\arcsin\left(\frac{\sin(\theta/2)}{2}\right) \\ \theta_3 &= \frac{\theta}{2} - \arcsin\left(\frac{\sin(\theta/2)}{2}\right). \end{aligned} \quad (4.10)$$

The *simultaneous* correction of pulse length errors and off-resonance effects is still being studied [52].

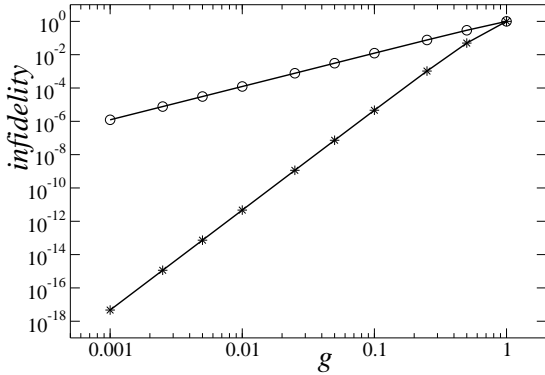


**Fig. 8.** The infidelity ( $1 - \mathcal{F}$ ) of simple and BB1 composite pulses to perform a NOT gate in the presence of a fractional pulse length error  $g$ ; note that both axes are plotted on log scales. The BB1 gate can achieve an infidelity of  $10^{-6}$  with an error in  $\omega_1$  of up to 10%, in contrast with the 0.1% accuracy required for a simple gate.

With any proposal for a “robust” gate it is vital to check that the errors take the form expected [55]. For a BB1 gate it is not necessary to get the absolute lengths of the pulses right, but it is essential to get the relative lengths correct. For a BB1 NOT gate ( $90_0^\circ 180_\phi^\circ 360_{3\phi}^\circ 180_\phi^\circ 90_0^\circ$ ) this is simple as all pulses are multiples of 90 degrees, but other cases may be more tricky. The BB1 gate also requires very accurate control of pulse phases, and it is likely that phase errors will dominate in experimental implementations.

#### 4.4 Two qubit gates

To obtain a complete set of robust gates it is also necessary to develop a family of robust two qubit gates, and the Ising coupling gate is the obvious choice [22]. The Ising gate is implemented by evolution under the Ising coupling Hamiltonian

$$\mathcal{H}_{IS} = \pi J 2I_z S_z \quad (4.11)$$

for a time  $\tau = \phi/\pi J$ , where  $J$  is the coupling strength and  $\phi$  is the desired evolution angle. In order to implement accurate controlled phase-shift gates it is necessary to know  $J$  with corresponding accuracy. Remarkably a very similar approach to that used for one qubit gates can also be used to tackle systematic errors in Ising coupling gates [56]; in effect Ising coupling corresponds to rotation about the  $2I_z S_z$  axis, and errors in  $J$  correspond to errors in a rotation angle about this axis. These can be parameterised by a

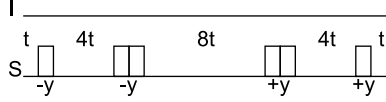


**Fig. 9.** Pulse sequence for an Ising gate to implement a controlled-NOT gate which is robust to small errors in  $J$ . Boxes correspond to single qubit rotations with rotation angles of  $\phi = \arccos(-1/8) \approx 97.2^\circ$  applied along the  $\pm y$  axes as indicated; time periods correspond to free evolution under the Ising coupling,  $\pi J 2I_z S_z$  for multiples of the time  $t = 1/4J$ . The naive Ising gate corresponds to free evolution for a time  $2t$ .

fractional error

$$\epsilon = \frac{J_{real}}{J_{nominal}} - 1. \quad (4.12)$$

and can be compensated by rotating about a sequence of axes tilted from  $2I_z S_z$  towards another axis, such as  $2I_z S_x$ . Defining

$$\theta_\phi \equiv \exp[-i \times \theta \times (2I_z S_z \cos \phi + 2I_z S_x \sin \phi)] \quad (4.13)$$

permits the naive sequence  $\theta_0$  to be replaced by a BB1 style sequence of the form

$$(\theta/2)_0 \pi_\phi 2\pi_{3\phi} \pi_\phi (\theta/2)_0 \quad (4.14)$$

with  $\phi = \arccos(-\theta/4\pi)$ . Note that the BB1 NOT gate described previously is simply a special case of this with  $\theta = \pi$ . The tilted evolutions are implemented by sandwiching a  $2I_z S_z$  rotation (evolution under the Ising Hamiltonian) between  $\phi_{\mp y}$  pulses applied to spin  $S$ . After combining and cancelling pulses the final sequence for the case  $\theta = \pi/2$  (which forms the basis of the controlled-NOT gate [22]) is shown in Fig. 9.

The BB1 Ising gate outperforms the naive gate much as before: once again the error is sixth order in  $g$ . The robust gate can tolerate errors in  $J$  of around 10% with an infidelity of  $10^{-6}$  [55, 56]. To perform a robust gate it is necessary to get the relative lengths of the coupling periods correct, but this is fairly simple as all times are multiples of  $1/4J$ . It is also important to use accurate pulses between the delays, but these can be achieved using robust single qubit gates.

#### 4.5 Suppressing weak interactions

This approach can easily be adapted to tackle another problem: developing a composite rotation which suppresses the effect of weak rotations. When converted to the two qubit equivalent, this gives a controlled phase-shift gate which effectively suppresses evolution under small Ising couplings [57]. This

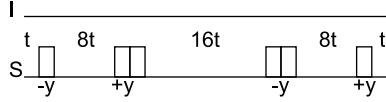


**Fig. 10.** Pulse sequence for a PB1 Ising gate to implement a controlled-NOT gate. Boxes are single qubit rotations with angles of  $\phi = \arccos(-1/16) \approx 93.6^\circ$ .

can be achieved using the same basic sequence as before, and comparing the composite quaternion with the null quaternion

$$\mathbf{q}_0 = \{1, \{0, 0, 0\}\} \quad (4.15)$$

and then using the Maclaurin series expansion around the point  $g = -1$ . The first order error terms can be removed by choosing  $\phi_2 = -\phi_1$  and  $\phi_1 = \arccos(-\theta/4\pi)$  as before.

Although derived independently, this sequence is in fact essentially identical to the NB1 composite rotation previously described by Wimperis [51]. The NB1 sequence does effectively suppress weak interactions, but this suppression is achieved at the cost of decreased robustness to small errors in strong interactions [57]. Clearly it would be desirable to gain similar suppression effects without this increased sensitivity to errors. Amazingly another composite rotation developed by Wimperis [51], this time called PB1, provides an excellent solution. This takes the form

$$(\theta/2)_x 360_{\phi_1} 720_{\phi_2} 360_{\phi_1} (\theta/2)_x \quad (4.16)$$

with  $\phi_2 = -\phi_1$  and  $\phi_1 = \arccos(-\theta/8\pi)$ . The pulse sequence for the two qubit version corresponding to a controlled-NOT gate is shown in Fig. 10 and its performance is compared with simple, BB1 and NB1 composite rotations in Fig. 11 This shows that the PB1 Ising gate outperforms a simple gate both in suppressing small couplings and in robustness to small errors in coupling strengths. If, however, only one of these effects is important, even better results can be obtained by using the NB1 or BB1 gate as appropriate.

## 5 An NMR miscellany

In this final section I will describe a variety of miscellaneous topics relevant to NMR quantum computers. In particular I will relax my previous restriction of considering only spin-half nuclei in liquids and solutions, and only spins systems beginning at thermal equilibrium.

### 5.1 Introduction

In the final lecture I will address a range of topics in the general field of NMR quantum computing. I will begin by describing how geometric

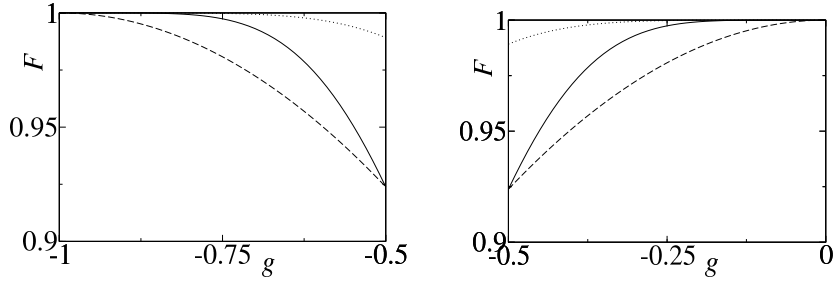


**Fig. 11.** Calculated fidelity of simple (dashed line), PB1 (solid line), and NB1 or BB1 (dotted line)  $90^\circ$  rotations as a function of the fractional error in the rotation rate  $g$ . The left hand plot shows the fidelity defined against the identity operation, with the dotted line showing the NB1 sequence; the right hand plot shows the fidelity defined against a  $90^\circ$  rotation, with the dotted line showing the BB1 sequence. Note that the horizontal axes differ in the two plots.

phases (Berry phases) can be used to implement logic gates in NMR systems [58]. I shall then consider the limits to NMR quantum computing [31], and whether these can be overcome with some of the more exotic schemes which have been suggested for performing NMR quantum computing, in particular those based on systems in the solid state or systems with nuclear spins greater than one half. Finally I shall discuss some of the non-Boltzmann methods which could in principle be used to perform initialisation of spin states, in particular those based on *para*-hydrogen.

## 5.2 Geometric phase gates

Classical geometric phases arise from motion of an object in a curved space [59]. For example, when an object is transported on the surface of a sphere, it can undergo a rotation arising solely from the curvature of the surface. Berrys phase [60], the simplest example of a geometric phase in quantum mechanics, arises in a quantum system when the Hamiltonian is varied adiabatically along a cyclic path. In NMR experiments it is usually simplest to apply a cyclic excursion to the Hamiltonian in the rotating frame. The two states of a spin-half nucleus will acquire equal and opposite geometric phases, in addition to any dynamic phases acquired during the evolution.

These geometric phases can be used to implement quantum logic gates [58]. This has the potential advantage that the Berry phase depends only on the geometry of the path, and not how it is traversed, and so should be insensitive to certain errors. Note, however, that a careful distinction should be made between *geometric* phase gates, such as those described here, and *topological* phase gates, which should exhibit extreme robustness



[61]. Topological phase gates are an exciting idea, but have not yet been demonstrated experimentally.

To see how geometric phases can be implemented in NMR, recall that off-resonance excitation gives rise to a Hamiltonian which is tilted in the rotating frame. The tilt angle can be controlled by varying the off-resonance fraction, which can be achieved either by changing the frequency offset or by changing the RF intensity. The phase angle can be controlled by simply changing the phase of the RF. Thus the Hamiltonian can be moved around the Bloch sphere at will. The simplest scheme is to begin by raising the RF intensity slowly from 0 up to some maximum value, so that the Hamiltonian is tilted away from the  $z$ -axis to some final tilt angle  $\theta$ , changing the phase of the RF so that the Hamiltonian rotates around a cone with cone angle  $\theta$ , and finally reducing the RF intensity back to zero. The geometric phases picked up during this process are

$$\pm\gamma = \pm\Omega/2 = \pm\pi(1 - \cos\theta) \quad (5.1)$$

where the  $\pm$  sign corresponds to the phase picked up by the  $\pm\frac{1}{2}$  spin states, which correspond to qubits in states  $|0\rangle$  and  $|1\rangle$ .

The geometric phase is most conveniently observed in NMR experiments by applying the adiabatic sweep to a spin in a superposition state, such as  $I_x$ ; the phases are then seen as a shift  $2\gamma$  in the *relative* phase of the superposition, that is as a  $2\gamma I_z$  rotation. However if the experiment is carried out as described the desired geometric phase will be completely swamped by the dynamic phase which arises simply from the integrated size of the Hamiltonian. Even worse, this dynamic phase will vary over the sample, as a result of RF inhomogeneity, and so when the final signal is averaged over the macroscopic ensemble the dynamic phase will cause extensive dephasing. It is, therefore, essential to refocus the dynamic phase, and as usual this can be achieved by using spin echoes: two adiabatic sweeps are applied with the second sweep sandwiched between a pair of  $180^\circ$  pulses. It might seem that the geometric phase would also be refocussed by this approach, but this can be overcome by reversing the direction of the phase rotation in the second sweep: the geometric term is reversed twice, and so adds up, while the dynamic term cancels out.

The description given so far has neglected the effects of spin–spin couplings. These can be assumed to take the Ising form, and so mean that the transition frequency of a spin depends on the spin state of its coupling partners. Thus the off-resonance frequency, the tilt angle, and so the geometric phase acquired, all depend on the state of the other spin (the control spin). (Note that in a heteronuclear spin system the control spin is very far from resonance and so not directly affected by the RF field.) The results of an experiment implementing this approach [58] are shown in Fig. 12. This shows the geometric phases acquired as a function of the maximum RF intensity

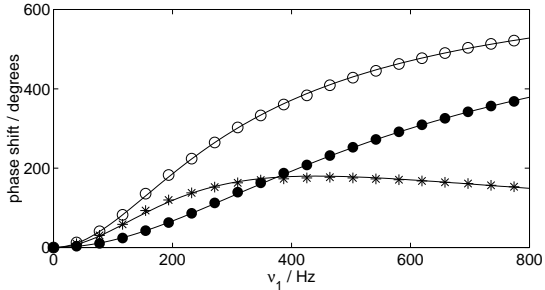


**Fig. 12.** Controlled geometric phases in  $^1\text{H}^{13}\text{CCl}_3$ . Filled and empty circles show the phase acquired by the  $^1\text{H}$  nucleus when the  $^{13}\text{C}$  nucleus is in  $|0\rangle$  and  $|1\rangle$ , while stars show the difference between these (the controlled phase); solid lines show theoretical predictions.

applied. As the maximum RF intensity is increased so are the cone angles, and thus the geometric phase acquired. More subtle behaviour is seen for the controlled geometric phase shift,  $\Delta\gamma$ , which first rises then falls. The extremely broad maximum in  $\Delta\gamma$  indicates that this is a robust method for generating differential phase shifts; the position and height of the maximum (here chosen to be  $180^\circ$ ) is determined by the average off-resonance frequency [58].

### 5.3 Limits to NMR quantum computing

Nuclear magnetic resonance is in many ways the leading quantum technology available to us for building small quantum computers [22]. Although it has been clear from the beginning that current NMR approaches are not scalable, and so cannot be used to build practical large scale devices, there is still substantial interest in the question of what the limits to NMR quantum computing really are.

The most commonly cited difficulty with current NMR approaches is their apparent inability to access pure initial states [38], leading to the use of non-scalable pseudo-pure state methods. This difficulty could in principle be overcome by using non-Boltzmann initial states [31], as described below. Note that schemes of this kind would also permit the creation of genuine entangled states, removing any concern about how “quantum” NMR approaches really are [39]. One serious problem might, however, remain: most of the non-Boltzmann schemes suggested would only allow the spin state to be initialised at the start of the computation; they would not allow the reinitialisation which lies at the heart of error correction schemes [34].

Another issue worth considering is the complexity of implementing pulse sequences with very large numbers of spins. This problem can be addressed

mathematically by determining how the number of pulses necessary to implement a logic gate scales with the size of the spin system; the development of efficient refocussing schemes [25, 26] means that the problem scales only quadratically, which is reasonable. It is also, however, important to consider practical questions, such as how individual qubits can be addressed. NMR quantum computing uses the different Larmor frequencies of different spins to achieve this, and this approach does not scale well, as the frequency space available is quite limited [31].

Finally it is necessary to consider issues of decoherence. Although NMR decoherence times can be extremely long compared with other techniques, what matters is not the absolute length of the decoherence time, but rather the ratio of the decoherence time to the gate time. Furthermore when estimating this number it is essential to use the time needed for the *slowest* gate in the system, which in NMR systems will correspond to the smallest coupling used. Experience to date suggests that NMR quantum computations are limited to around 500 gates before the effects of decoherence become overwhelming [50, 62]. Note that this number lies well below the value required for effective error correction schemes [34].

Putting all these issues together, it seems that the limit to current NMR approaches lies around 10–15 qubits. While this is far beyond the abilities of any currently competing technology, it is not enough to make NMR a practical quantum technology.

#### 5.4 *Exotica*

Throughout these lectures NMR has been used to refer solely to studies of spin-half nuclei in liquids and solutions. This restricted field dominates both conventional NMR studies and NMR implementations of quantum computing for a number of related reasons. There is an obvious way to map qubits onto spin-half nuclei, and the spin-half Hamiltonian in the liquid state takes a particularly nice form, which is powerful enough to be computationally universal, but simple enough to be easy to work with. Experience from conventional NMR means that the field is extremely well understood, and the available technology is highly sophisticated. It is, however, worth briefly relaxing these restrictions and seeing what the rest of NMR might have to offer.

Studying spin-half nuclei in the solid state [12] appears to have many advantages. The solid state permits access to very low temperatures, and so the preparation of pure initial states by simple Boltzmann means. This does not, however, solve the detection problem, or provide a method of reinitialisation. Solid state samples also retain the full dipolar coupling Hamiltonian, which is much larger than the isotropic scalar coupling, and so should allow much faster gates. On the down side, however, dipolar coupling networks are much more extended than scalar coupling networks,

as the dipolar coupling falls off only slowly with distance. Furthermore the homonuclear dipole-dipole coupling Hamiltonian is not truncated to the (convenient) Ising form. These effects make multiplets extremely broad, rendering selective excitation of individual qubits difficult or impossible. One extreme possibility which has been suggested is to adopt techniques from magnetic resonance imaging to select spins according to their positions in space, but implementing this will not be easy.

Between liquid and solid state NMR lies the study of molecules in liquid crystal solvents. These combine some of the features of both extremes, and in particular give some access to dipole-dipole couplings in a controlled manner. This approach has been used in implementations of NMR quantum computing [63,64], but while intriguing it is unlikely to prove important.

Another possibility which has been suggested is to use nuclei with spin greater than one half, usually in the solid state. Such nuclei have *both* a magnetic dipole moment *and* a nuclear quadrupole moment, and are often called quadrupolar nuclei [12]. The quadrupole moment will interact with electric field gradients, and the behaviour of quadrupolar nuclei is dominated by the interplay between this interaction and the interaction with magnetic fields. This can become quite complex, as the relative importance of the two interactions varies greatly for different nuclei and for different chemical environments, and the electric field gradient and magnetic field are usually attached to quite different reference frames. While this interplay could, in principle, be useful, it can also lead to many difficulties, the most obvious example being rapid dephasing.

Quadrupolar nuclei also have more than two spin states, which obviously suggests using one spin to store more than one qubit. It is in principle possible to build a two-qubit device in a single nucleus with spin- $\frac{3}{2}$ , or even a three-qubit device in a spin- $\frac{7}{2}$  nucleus. The problem with this approach is, of course, that it does not scale beyond three qubits.

Going beyond nuclei, electrons are spin-half particles, and it should be possible to perform NMR like experiments using electron spin resonance, or ESR, studies of unpaired electrons in radicals [65]. (ESR is sometimes known as electron paramagnetic resonance, or EPR.) The electron magnetic moment is much larger than nuclear moments, and so ESR is usually a microwave technique. This also means that pure spin states could be reached by cooling to the temperature of liquid helium. The theory of ESR looks very similar to that of NMR, but the experiments are as yet much less developed. Another problem is that radicals with multiple unpaired electrons are very rare, and for this reason most proposals have concentrated on artificial nanostructures. Although this field will be challenging, it is certainly worth a look.

In the long term one of the most promising techniques is ENDOR, or electron nuclear double resonance [66], which combines NMR and ESR tech-

niques. NMR and ESR have very different energy scales, which makes the experiments tricky, but may also prove very useful, allowing the high energy scale of ESR to be used for quantum gates, and the low energy scale of NMR to be used for storage. This is, of course, the ultimate basis of the Kane proposal for a large scale quantum computer [67].

### 5.5 *Non-Boltzmann initial states*

Although the problem of initialisation is not the only factor limiting NMR implementations of quantum computing, it remains an important and annoying problem. The low polarisation of Boltzmann states is also an important issue in conventional NMR studies, as it results in a low signal strength, greatly limiting the sensitivity of NMR as an analytical technique. For this reason there has long been interest in developing ways to enhance NMR polarisations, and many different techniques have been developed [31]. Of these, however, only two have any realistic prospect of preparing essentially pure states: optical pumping, and the use of *para*-hydrogen.

Optical pumping is, of course, widely used to prepare atoms and ions in desired electronic states, and these techniques can be extended to prepare essentially pure nuclear spin states. Two systems dominate optically pumped NMR:  $^3\text{He}$ , which can be pumped directly, and  $^{129}\text{Xe}$  and  $^{131}\text{Xe}$ , which are pumped indirectly via rubidium atoms. In both cases it is possible to achieve extremely high polarisations, close to unity. However these near pure spin states are almost useless for quantum computing, as each atom can only hold one qubit (or two in the case of the quadrupolar nucleus  $^{131}\text{Xe}$ ), and the atoms do not interact to form molecules. It is possible in principle to transfer these high polarisations to other nuclei [68], but so far the efficiency of such transfers has been too low to be useful.

An intriguing alternative is provided by *para*-hydrogen. This relies on the fact that the rotational and nuclear spin states of homonuclear diatomic molecules such as hydrogen are inextricably connected by the Pauli principle; in particular the even rotational states of hydrogen must have anti-symmetric nuclear spin states. Cooling hydrogen to the rotational ground state would give pure *para*-hydrogen with a singlet spin state. As the inter-conversion of *ortho* and *para*-hydrogen is forbidden, it is necessary to use a catalyst, but this means that the enhancement will be retained on warming if the catalyst is removed. Thus it is possible to obtain a bottle of hydrogen gas at room temperature with essentially pure nuclear spin states!

It is, of course, not possible to implement quantum computing with *para*-hydrogen directly because the hydrogen molecule is too symmetric: it is essential to break the symmetry so that the two nuclei can be addressed individually. This is easily achieved by adding the *para*-hydrogen to some other molecule, such as Vaska's catalyst, to produce a complex where the two

$^1\text{H}$  nuclei have different chemical shifts and so can be separately addressed [69–71]. The addition reaction occurs with retention of nuclear spin state, and so the purity is conserved. In most studies to date, however, the reaction occurs quite slowly in comparison with the Zeeman frequency difference of the two spins, leading to dephasing of the off-diagonal elements of the density matrix, converting the singlet state to an incoherent mixture of  $|01\rangle$  and  $|10\rangle$ . In conventional *para*-hydrogen studies this dephasing is accepted, but for NMR quantum computing it is necessary to have fully coherent addition. One approach used to date [72] is to apply an *isotropic mixing* pulse sequence [3], such as MLEV-16, which removes the dephasing Zeeman interaction and preserves the pure singlet spin state. Early experiments using this approach have achieved a purity of around 10% in a two qubit system [72], significantly below the entanglement threshold. A more recent experiment has generated systems with a purity of around 86% [73].

## 6 Summary

Nuclear Magnetic Resonance (NMR) is arguably both the best and the worst technology we have for the implementation of small quantum computers. Its strengths lie in the ease with which arbitrary unitary transformations can be implemented, and the great experimental simplicity arising from the low energy scale and long time scale of radio frequency transitions; its weaknesses lie in the difficulty of implementing essential non-unitary operations, most notably initialisation and measurement.

The debate over whether NMR quantum computers are “real” quantum computers has generated much heat, but also some useful light. It is now clear that NMR is indeed quantum mechanical, and can in principle be used to build quantum computers, but that the current approach based on pseudo-pure states will never lead to true quantum computing.

Current NMR techniques are not a serious candidate for real quantum computing, but NMR remains a great technique for playing around with small numbers of qubits. The unparalleled sophistication of NMR will almost certainly prove a rich source of insights which will find their ultimate applications in other fields.

## A Commutators and product operators

The product operator formalism allows the behaviour of spin systems undergoing complicated NMR pulse sequences to be calculated using nothing more than elementary trigonometry and a table of commutators. A table of the most important commutators in a two spin system is given below. As an example consider the element in the row labelled  $I_x$  and the column labelled  $I_z$ ; the commutator  $[I_x, I_z] = -iI_y$  and this is entered in the table.

	$I_x$	$I_y$	$I_z$	$S_x$	$S_y$	$S_z$	$2I_z S_z$
$I_x$	0	$+iI_z$	$-iI_y$	0	0	0	$-i2I_y S_z$
$I_y$	$-iI_z$	0	$+iI_x$	0	0	0	$+i2I_x S_z$
$I_z$	$+iI_y$	$-iI_x$	0	0	0	0	0
$S_x$	0	0	0	0	$+iS_z$	$-iS_y$	$-i2I_z S_y$
$S_y$	0	0	0	$-iS_z$	0	$+iS_x$	$+i2I_z S_x$
$S_z$	0	0	0	$+iS_y$	$-iS_x$	0	0
$2I_x S_x$	0	$+i2I_z S_x$	$-i2I_y S_x$	0	$+i2I_x S_z$	$-i2I_x S_y$	0
$2I_x S_y$	0	$+i2I_z S_y$	$-i2I_y S_y$	$-i2I_x S_z$	0	$+i2I_x S_x$	0
$2I_x S_z$	0	$+i2I_z S_z$	$-i2I_y S_z$	$-i2I_x S_y$	$+i2I_x S_x$	0	$-iI_y$
$2I_y S_x$	$-i2I_z S_x$	0	$+i2I_x S_x$	0	$+2iI_y S_z$	$-i2I_y S_y$	0
$2I_y S_y$	$-i2I_z S_y$	0	$+i2I_x S_y$	$-i2I_y S_z$	0	$+i2I_y S_z$	0
$2I_y S_z$	$-i2I_z S_z$	0	$+i2I_x S_z$	$+i2I_y S_y$	$-i2I_y S_x$	0	$+iI_x$
$2I_z S_x$	$+i2I_y S_x$	$-i2I_x S_x$	0	0	$+i2I_z S_z$	$-i2I_z S_y$	$-iS_y$
$2I_z S_y$	$+i2I_y S_y$	$-i2I_x S_y$	0	$-i2I_z S_z$	0	$+i2I_z S_x$	$+iS_x$
$2I_z S_z$	$+i2I_y S_z$	$-i2I_x S_z$	0	$+i2I_z S_y$	$-i2I_z S_x$	0	0

From this element one can immediately deduce that

$$I_x \xrightarrow{\theta I_z} I_x \cos \theta + I_y \sin \theta.$$

In the same way the next element in the table can be used to deduce that  $I_x$  commutes with  $S_x$ , and so

$$I_x \xrightarrow{\theta S_x} I_x.$$

These rules permit easy calculation of the evolution of any state of a two spin system under any one of the product operators found in simple Hamiltonians, but real Hamiltonians will contain several terms at once: for example the weak coupling Hamiltonian of a two spin system contains terms proportional to  $I_z$ ,  $S_z$  and  $2I_z S_z$ . When, as in this case, the terms all commute the situation is simple, and the total evolution can be calculated by applying the terms sequentially in any desired order. A similar situation occurs when pulses are applied simultaneously to two or more spins: as one-spin operators on different spins all commute the pulses can be applied separately. Note, however, that pulse Hamiltonians do *not* commute with the background Hamiltonian, and it is necessary to neglect this during pulses: this is a good approximation for short high power hard pulses. In the same way the three components contributing to a Heisenberg coupling ( $2I_x S_x$ ,  $2I_y S_y$ , and  $2I_z S_z$ ) do not commute, and so the product operator approach can only be used in the weak coupling regime where the Heisenberg coupling is truncated to the Ising ( $2I_z S_z$ ) form.

## References

- [1] A. Abragam. *Principles of Nuclear Magnetism*. Clarendon Press, Oxford, UK, 1961.
- [2] R. R. Ernst, G. Bodenhausen, and A. Wokaun. *Principles of Nuclear Magnetic Resonance in One and Two Dimensions*. Clarendon Press, Oxford, UK, 1987.
- [3] R. Freeman. *Spin Choreography: Basic Steps in High Resolution NMR*. Spektrum, Oxford, UK, 1997.
- [4] M. Goldman. *Quantum Description of High-Resolution NMR in Liquids*. Clarendon Press, Oxford, UK, 1988.
- [5] P. J. Hore. *Nuclear Magnetic Resonance*. Oxford Chemistry Primers, Oxford, UK, 1995.
- [6] M. H. Levitt. *Spin Dynamics: Basics of Nuclear Magnetic Resonance*. Wiley, Chichester, UK, 2001.
- [7] R. Freeman. *Magnetic Resonance in Chemistry and Medicine*. Oxford University Press, Oxford, UK, 2003.
- [8] T. Claridge. *High-resolution NMR Techniques in Organic Chemistry*. Pergamon, 1999.
- [9] R. Freeman. *A Handbook of Nuclear Magnetic Resonance*. Longman, Harlow, UK, 1987.
- [10] O. W. Sørensen, G. W. Eich, M. H. Levitt, G. Bodenhausen, and R. R. Ernst. *Prog. Nucl. Magn. Reson. Spectrosc.*, 16:163–192, 1983.
- [11] P. J. Hore, J. A. Jones, and S. Wimperis. *NMR: The Toolkit*. Oxford Chemistry Primers, Oxford, UK, 2000.
- [12] K. Schmidt-Rohr and H. W. Spiess. *Multidimensional Solid-State NMR and Polymers*. Academic Press, San Diego, CA, 1994.
- [13] E. L. Hahn. *Phys. Rev. Lett.*, 80:580, 1950.
- [14] D. P. DiVincenzo. *Proc. Roy. Soc. Lond. A*, 454:261–276, 1998.
- [15] D. Deutsch. *Proc. Roy. Soc. Lond. A*, 425:73–90, 1989.
- [16] D. Deutsch, A. Barenco, and A. Ekert. *Proc. Roy. Soc. Lond. A*, 449:669–677, 1995.
- [17] A. Barenco, C. H. Bennett, R. Cleve, D. P. DiVincenzo, N. Margolus, P. Shor, T. Sleator, J. A. Smolin, and H. Weinfurter. *Phys. Rev. A*, 52:3457–3467, 1995.
- [18] A. Barenco. *Proc. Roy. Soc. Lond. A*, 449:679–683, 1995.
- [19] D. G. Cory, A. F. Fahmy, and T. F. Havel. In T. Toffoli, M. Biafore, and Leão, editors, *Proceedings of Phys Comp '96*, pages 87–91. New England Complex Systems Institute, 1996.
- [20] D. G. Cory, A. F. Fahmy, and T. F. Havel. *Proc. Natl. Acad. Sci. USA*, 64:1634–1639, 1997.
- [21] N. A. Gershenfeld and I. L. Chuang. *Science*, 275:350–356, 1997.
- [22] J. A. Jones. *Prog. Nucl. Magn. Reson. Spectrosc.*, 38:325–360, 2001.
- [23] R. Freeman, T. A. Frenkiel, and M. H. Levitt. *J. Magn. Reson.*, 44:409–412, 1981.
- [24] E. Knill, R. Laflamme, R. Martinez, and C. H. Tseng. *Nature*, 404:368–370, 2000.
- [25] J. A. Jones and E. Knill. *J. Magn. Reson.*, 141:322–325, 1999.
- [26] D. W. Leung, I. L. Chuang, F. Yamaguchi, and Y. Yamamoto. *Phys. Rev. A*, 61:042310, 2000.
- [27] J. A. Jones and M. Mosca. *Phys. Rev. Lett.*, 83:1050–1053, 1999.
- [28] N. Linden, H. Barjat, and R. Freeman. *Chem. Phys. Lett.*, 296:61–67, 1998.
- [29] P. Zanardi and M. Rasetti. *Phys. Rev. Lett.*, 79:3306–3309, 1997.
- [30] L. Viola, E. M. Fortunato, M. A. Pravia, E. Knill, R. Laflamme, and D. G. Cory. *Science*, 93:2059–2063, 2001.



- [31] J. A. Jones. *Fort. der Physik*, 48:909–924, 2000.
- [32] S. L. Braunstein and H. K. Lo, editors. *Scalable Quantum Computers: Paving the Way to Realisation*. Wiley, 2001.
- [33] J. A. Jones and M. Mosca. *J. Chem. Phys.*, 109:1648–1653, 1998.
- [34] A. M. Steane. *Phil. Trans. Roy. Soc. Lond. A*, 356:1739–1758, 1998.
- [35] J. A. Jones. *PhysChemComm*, 11, 2001.
- [36] J. A. Jones, R. H. Hansen, and M. Mosca. *J. Magn. Reson.*, 135:353–360, 1998.
- [37] E. Knill, I. Chuang, and R. Laflamme. *Phys. Rev. A*, 57:3348–3363, 1998.
- [38] W. S. Warren. *Science*, 277:1688–1689, 1997.
- [39] S. L. Braunstein, C. M. Caves, R. Jozsa, Lindenn N., S. Popescu, and R. Schack. *Phys. Rev. Lett.*, 83:1054–1057, 1999.
- [40] N. Linden and S. Popescu. *Phys. Rev. Lett.*, 87:047901, 2001.
- [41] R. Schack and C. M. Caves. *Phys. Rev. A*, 60:4354–4362, 1999.
- [42] E. Knill and R. Laflamme. *Phys. Rev. Lett.*, 81:5672–5675, 1998.
- [43] L. J. Schulman and U. Vazirani. In *Proc. 31st ACM STOC*, pages 322–329, 1999. E-print quant-ph/9804060.
- [44] H. K. Cummins, C. Jones, A. Furze, N. Soffe, M. Mosca, J. M. Peach, and J. A. Jones. *Phys. Rev. Lett.*, 88:187901, 2002.
- [45] W. K. Woiters and W. H. Zurek. *Nature*, 299:802–803, 1982.
- [46] V. Bužek and M. Hillery. *Phys. Rev. A*, 54:1844–1852, 1996.
- [47] M. H. Levitt and R. Freeman. *J. Magn. Reson.*, 33:473, 1979.
- [48] M. H. Levitt. *Prog. Nucl. Magn. Reson. Spectrosc.*, 18:61–122, 1986.
- [49] M. D. Bowdrey, D. K. L. Oi, A. J. Short, K. Banaszek, and J. A. Jones. *Phys. Lett. A*, 294:258–260, 2002.
- [50] H. K. Cummins and J. A. Jones. *New J. Phys.*, 2:1–12, 2000.
- [51] S. Wimperis. *J. Magn. Reson. A*, 109:221–231, 1994.
- [52] H. K. Cummins, G. Llewellyn, and J. A. Jones. *Phys. Rev. A*, 67:042308, 2003.
- [53] R. Tycko. *Phys. Rev. Lett.*, 51:775, 1983.
- [54] H. K. Cummins and J. A. Jones. *Contemp. Phys.*, 41:383–399, 2000.
- [55] J. A. Jones. *Phil. Trans. Roy. Soc. Lond. A*, 361:1429–1440, 2003.
- [56] J. A. Jones. *Phys. Rev. A*, 67:012317, 2003.
- [57] J. A. Jones. *Phys. Lett. A*, 316:24–28, 2003.
- [58] J. A. Jones, V. Vedral, G. Ekert, and G. Castagnoli. *Nature*, 403:869–871, 2000.
- [59] A. Shapere and F. Wilczek, editors. *Geometric Phases in Physics*. World Scientific, Singapore, 1989.
- [60] M. V. Berry. *Proc. Roy. Soc. Lond. A*, 392:45, 1984.
- [61] A. Y. Kitaev. *Annals Phys.*, 303:2–30. E-print quant-ph/9707021.
- [62] L. M. K. Vandersypen, M. Steffen, G. Breyta, C. S. Yannoni, M. H. Sherwood, and I. L. Chuang. *Nature*, 414:883–887, 2001.
- [63] M. Marjanska, I. L. Chuang, and M. G. Kubinec. *J. Chem. Phys.*, 112:5095–5099, 2000.
- [64] B. M. Fung. *J. Chem. Phys.*, 115:8044–8048, 2001.
- [65] A. Schweiger and G. Jeschke. Oxford University Press, Oxford, UK, 2001.
- [66] M. Mehring, J. Mende, and W. Scherer. *Phys. Rev. Lett.*, 90:153001, 2003.
- [67] B. E. Kane. *Nature*, 393:133–137, 1998.
- [68] A. S. Verhulst, O. Liivak, M. H. Sherwood, H. Vieth, and I. L. Chuang. *Appl. Phys. Lett.*, 79:2480–2482, 2001.

- [69] C. R. Bowers and D. P. Weitekamp. *Phys. Rev. Lett.*, 57:2645–2648, 1986.
- [70] J. Natterer and J. Bargon. *Prog. Nucl. Magn. Reson. Spectrosc.*, 31:293–315, 1997.
- [71] S. B. Duckett and C. J. Sleigh. *Prog. Nucl. Magn. Reson. Spectrosc.*, 34:71–92, 1999.
- [72] P. Hübler, J. Bargon, and S. J. Glaser. *J. Chem. Phys.*, 113:2056–2059, 2000.
- [73] M. S. Anwar *et al.* unpublished results, 2003.